Quasiclassical calculation of magnetoresistance oscillations of a two-dimensional electron gas in spatially periodic magnetic and electrostatic fields

Rolf R. Gerhardts

Max-Planck-Institut für Festkörperforschung, Heisenbergstrasse 1, D-70569 Stuttgart, Federal Republic of Germany
(Received 14 December 1995)

A classical approach, relating magnetoresistance oscillations of a two-dimensional electron gas (2DEG) in a weak lateral superlattice to the guiding center drift of cyclotron orbits, is extended to superlattices defined by spatially periodic electrostatic and magnetic fields of arbitrary shape but equal lattice constants. The results are applied to the experimentally relevant situation of modulation fields produced by periodic arrays of magnetized strips or dots on the surface of a heterostructure containing a 2DEG. Magnetic modulation fields of different symmetries, tuned by the orientation of the magnetization, are superimposed on the stress-induced electrostatic modulation and lead to characteristic interference effects on the Weiss oscillations of the magnetoresistance.

I. INTRODUCTION

A two-dimensional electron gas (2DEG) subjected to a perpendicular homogeneous magnetic field and weak spatially periodic modulation fields, shows interesting commensurability effects. In magnetic fields of intermediate strengths, these are manifested in the so-called Weiss oscillations of the magnetoresistance, which have first been observed in 2DEG's in $Al_{1-x}Ga_xAs$-GaAs heterostructures with a weak *electrostatic* modulation.[1] The Weiss oscillations have been understood[2,3] within a quantum mechanical picture, as resulting from the modulation-induced broadening of the Landau levels into Landau bands, with an oscillatory dependence of the bandwidth on the Landau quantum number. The dispersion of the Landau bands leads to a group velocity, and this to a "band conductivity," which both vanish when the Landau levels become flat. This happens when "flat-band conditions" hold which, for large Landau quantum numbers, can be expressed by simple ratios of the cyclotron radius at the Fermi energy of the 2DEG and the period of the modulation potential. Although some aspects of the Weiss oscillations, notably in 2D lateral superlattices, seem to require a quantum mechanical explanation (for a review see Ref. 4), other aspects can be understood within a simple quasiclassical approach,[5,6] in which the analog of the quantum mechanical group velocity appears as a drift velocity of the guiding centers of cyclotron orbits in the crossed homogeneous magnetic field and the periodic electric field of the modulation.

The analog of the Weiss oscillations in a 2DEG with a 1D lateral superlattice defined by a *periodic magnetic field* was predicted[7] and investigated in some detail[8,9] several years ago. The experimental realization of these superlattices and the observation of the predicted effect has, however, been achieved only recently.[10–12] The magnetic modulation has been produced by metallic strips on the surface, consisting either of superconducting[10] or ferromagnetic[11,12] material. Whereas the flux expulsion by the superconductor leads to tiny modulation effects, the deposition of dysprosium (Dy) micromagnets on the surface leads to very strong modulation effects.[11] Since the thermal expansion coefficients of the

metal and of the semiconductor heterostructure are different, the ferromagnetic strips exert, at the low temperatures of the experiment, mechanical stress on the underlying semiconductor, which leads to a periodic modulation of the conduction band edge and acts as an electrostatic modulation on the 2DEG. This stress effect has been investigated systematically,[13,14] and it has been found that this unavoidable electrostatic modulation has a considerable content of higher harmonics. For the understanding of the magnetic Weiss oscillations, it is important to be aware of the fact that this stress-induced modulation is always present.[11]

A quantum mechanical study of the Weiss oscillations in the presence of both an electrical and a magnetic modulation in one lateral direction has been presented by Peeters and Vasilopoulos.[9] This study has been restricted to purely sinusoidal modulations in the two special cases that either the cosine modulation of the magnetic field is in phase with that of the electrostatic potential, or that there is a phase difference of $\pi/2$ between these.

The purpose of the present paper is twofold. First, we want to demonstrate that for one- and two-dimensional lateral superlattices, under conditions which can be realized experimentally,[15] a rich variety of interesting interference effects exists in which the stress-induced modulation acts together with a magnetic modulation. Situations of very different symmetries can be generated, since the strength and the phase of the magnetic modulation can be tuned via the strength and the direction of the magnetization of the micromagnets on the surface. Second, we want to generalize a simple classical approach,[5,6] based on the calculation of the guiding center drift of the cyclotron orbits in a weak magnetoelectric modulation, which then allows us to calculate the Weiss oscillations of the magnetoresistance in such situations, including the case of strongly anharmonic periodic modulations. We will demonstrate that the higher harmonics may give rise to nondiagonal contributions to the resistance tensor, which are entirely absent in the simple harmonic approximation.

The plan of this paper is as follows. In Sec. II and the Appendices we calculate the guiding-center drift velocities as well as the formula for the corrections to the Drude resis-

tivity tensor, due to this drift, to lowest order in the modulation amplitudes. In Sec. III we apply this formula to typical situations, paying special attention to reasonable treatment of the modulation fields generated by periodic arrays of micromagnets on the surface of the sample.

II. QUASICLASSICAL BAND CONDUCTIVITY

A. Guiding-center drift

Within the semiclassical picture, the Weiss oscillations of the magnetoresistance of a two-dimensional electron gas in a lateral superlattice, realized by a weak electrostatic potential modulation, is related to the drift motion of cyclotron orbits. Without modulation, the homogeneous magnetic field $\vec{B}_0$ applied perpendicularly to the plane of the 2DEG forces the electrons on circular orbits of radius R_c and energy $\frac{m}{2}\omega_c^2 R_c^2$, with $\omega_c = eB_0/mc$ the cyclotron frequency. We consider only electrons at the Fermi energy $E_F = \hbar^2 k_F^2/2m$, so that $R_c = v_F/\omega_c$, with $v_F = \hbar k_F/m$ the Fermi velocity. If the modulation is sufficiently weak, it will lead only to a minor modification of the cyclotron orbits, notably a drift of their center coordinates or ''guiding'' centers.

In order to calculate the average drift velocity $\vec{v}^D$ of the guiding center of a cyclotron orbit, we start with Newton's equation of motion for the velocity $\vec{v} = \dot{\vec{r}}$ of an electron in the x-y plane,

$$m\dot{\vec{v}} = -e[\vec{E} + (\vec{v}/c) \times \vec{B}], \qquad (2.1)$$

with an in-plane electric field $\vec{E} = \nabla V(\vec{r})/e$, expressed in terms of the potential energy $V(\vec{r})$ of the electron of charge $-e < 0$, and a perpendicular magnetic field $\vec{B} = (0,0,B_0 + B_m(\vec{r}))$. We assume that $V(\vec{r})$ and $B_m(\vec{r})$ are periodic on the same rectangular lattice with lattice constants $a_x = 2\pi/K_x$ and $a_y = 2\pi/K_y$,

$$V(\vec{r}) = \sum_{q \neq 0} V_{\vec{q}} e^{i\vec{q}\cdot\vec{r}}, \quad B_m(\vec{r}) = \sum_{q \neq 0} B_{\vec{q}} e^{i\vec{q}\cdot\vec{r}}, \qquad (2.2)$$

and that they have zero average values, so that, in Eq. (2.2), the $\vec{q}$ sums are over $\vec{q} = (K_x n_x, K_y n_y, 0)$ with integers n_x and n_y which are not simultaneously zero.

In the absence of modulations, the solution $\vec{r} = (x(\varphi), y(\varphi), 0)$ of Eq. (2.1) reads

$$x(\varphi) = x_M + R_c \sin\varphi, \quad y(\varphi) = y_M - R_c \cos\varphi, \qquad (2.3)$$

with $\varphi = \omega_c t + \varphi_0$, and the guiding-center coordinates

$$x_M = x - v_y/\omega_c, \quad y_M = y + v_x/\omega_c \qquad (2.4)$$

are constant in time.

In the presence of modulations, we define the guiding center for each point on a modified cyclotron orbit as the center of the circle of curvature at that point. As is shown in Appendix A, we obtain results for the drift velocity of the guiding centers, which are correct to first order in the modulation fields, if we first take Eq. (2.4) as the definition for the guiding center and calculate its velocity from Eq. (2.1),

$$\dot{x}_M = c\frac{E_y}{B_0} - v_x\frac{\omega_m}{\omega_c}, \quad \dot{y}_M = -c\frac{E_x}{B_0} - v_y\frac{\omega_m}{\omega_c} \qquad (2.5)$$

and, secondly, calculate the average drift velocity by averaging Eq. (2.5) along an unperturbed cyclotron orbit (2.3),

$$v_x^D = \int_{-\pi}^{\pi} \frac{d\varphi}{2\pi} \left[\frac{c}{B_0} E_y(\vec{r}(\varphi)) - R_c \omega_m(\vec{r}(\varphi))\cos\varphi \right], \quad (2.6)$$

$$v_y^D = \int_{-\pi}^{\pi} \frac{d\varphi}{2\pi} \left[-\frac{c}{B_0} E_x(\vec{r}(\varphi)) - R_c \omega_m(\vec{r}(\varphi))\sin\varphi \right]. \qquad (2.7)$$

Here $\omega_m(\vec{r}) = eB_m(\vec{r})/mc$ is defined in analogy to ω_c, and v_x^D and v_y^D depend on the radius R_c and the center position $\vec{r}_M$ of the selected orbit. To evaluate these integrals, we insert the Fourier expansions (2.2) and obtain after a straightforward calculation

$$\vec{v}^D = \frac{i}{m\omega_c} \sum_{q \neq 0} \vec{g}(\vec{q}) e^{i\vec{q}\cdot\vec{r}_M} \mathscr{S}_{\vec{q}}, \qquad (2.8)$$

in which $\vec{g}(\vec{q}) = (q_y, -q_x, 0)$ and

$$\mathscr{S}_{\vec{q}} = \sigma_{B_0} V_{\vec{q}} J_0(R_c q) + \frac{k_F}{q} \hbar \omega_{\vec{q}} J_1(R_c q), \qquad (2.9)$$

with $\sigma_{B_0} = B_0/|B_0|$, $q = |\vec{q}|$, $\omega_{\vec{q}} = eB_{\vec{q}}/mc$, and $J_\nu(x)$ the Bessel functions of the first kind. So far we have tacitly assumed that the homogeneous part of the magnetic field points into the positive z direction, i.e., $\vec{B}_0 = B_0\vec{e}_z$ with $B_0 > 0$, so that $\sigma_{B_0} = 1$.

It is interesting to keep the modulations of the electrostatic potential and of the magnetic field fixed and to invert the direction of the homogeneous magnetic field, i.e., to take $B_0 < 0$. Then the electrons move through the cyclotron orbits in the opposite direction, so that at each point of the orbit the velocity has the opposite sign. Formally, the consequences for the average guiding center drift are seen most easily form Eq. (2.5). The first term, i.e., the usual $(\vec{E} \times \vec{B}_0)/B_0^2$ drift, changes sign with B_0. The second drift term $-\vec{v}B_m/B_0$, due to the magnetic modulation, remains, however, unchanged, since together with B_0 the velocity $\vec{v}$ changes sign. As a consequence, if we take ω_c and R_c in Eqs. (2.8) and (2.9) to be positive, we have $\sigma_{B_0} = -1$ for $B_0 < 0$. This result is also easily understood from the disturbed cyclotron orbits. An electric modulation in the x direction leads to cycloidic orbits which drift in the y direction, with local radius of curvature $R_c(x) = \{2[E_F - V(x)]/m\}^{1/2}/\omega_c$. When the direction of B_0 is inverted, the electron follows the same orbit in opposite direction, and the drift velocity changes sign. A magnetic modulation in the x direction with $|B_m(x)| < |B_0|$ leads to a similar orbit with local radius $R_c(x) = (2mE_F)^{1/2}c/[e|B_0 + B_m(x)|]$. When the direction of B_0 is inverted, the orbit changes. Regions corresponding to large values of $R_c(x)$ are interchanged with those corresponding to smaller values, but the electron also travels locally in the opposite direction, so that the overall drift velocity remains unchanged.

B. Contribution to conductivity

The guiding-center drift introduces a degree of freedom in addition to the cyclotron motion, so that an additional contribution to the velocity-velocity correlation function and, therefore, to the diffusion tensor appears. The corresponding contribution to the conductivity tensor, which adds to the usual Drude conductivity, can be written in the form

$$\Delta \sigma_{\mu\nu} = \frac{\tau e^2 m}{\pi \hbar^2} \langle v_\mu^D v_\nu^D \rangle_{\text{u.c.}}, \quad (2.10)$$

where the contribution of the individual cyclotron orbits must be averaged with respect to their center coordinates $\vec{r}_M$ over the unit cell of the superlattice.[5,6] As shown in Appendix B, Eq. (2.10) follows from the more familiar expression for the conductivity in terms of the velocity-velocity correlation function when the relaxation time τ is much larger than the period of the cyclotron motion, i.e., for $\omega_c \tau \gg 1$. According to Eq. (2.8), the integral with respect to $\vec{r}_M$ reduces the double sum, introduced by the product of two components of the drift velocity, to a single $\vec{q}$ sum. This yields for the ''band conductivity'' tensor

$$\Delta \sigma_{\mu\nu} = \frac{\tau e^2}{\pi m (\hbar \omega_c)^2} \sum_{\vec{q} \neq 0} g_\mu(\vec{q}) g_\nu(\vec{q}) |\mathscr{S}_{\vec{q}}|^2, \quad (2.11)$$

which generalizes a previous result[6,4] for purely electrostatic modulation.

C. Comparison with previous calculations

Results similar to Eq. (2.11) but for simple sinusoidal modulations in only one direction have been obtained by other authors.[8,9] We want to compare explicitly with the result of a quantum mechanical calculation by Peeters and Vasilopoulos[9] for $V(x) = V_0 \cos Kx$ and $B_m(x) = B_m \cos Kx$, and for one spin direction. With slightly altered notation, Eq. (22) of Ref. 9 reads

$$\sigma_{yy}^{\text{dif}} \approx \frac{e^2 \tau K^2 l^2}{4 \pi \hbar^2} \sum_n [W_n(u)]^2 \left(-\frac{\partial f(E)}{\partial E} \right)_{E=E_n}, \quad (2.12)$$

with $l = (\hbar/m\omega_c)^{1/2}$ the magnetic length, $u = K^2 l^2/2$, and with $W_n(u) = |V_0 F_n(u) + \hbar \omega_m G_n(u)|$ the half width of the nth Landau level. Here $G_n(u) = -\partial F_n(u)/\partial u$ and $F_n(u) = \exp(-u/2) L_n(u)$ with $L_n(u)$ a Laguerre polynomial. To compare with our quasiclassical calculation, we first note that our averaging over cyclotron orbits is only meaningful if the relaxation time τ is sufficiently large, i.e., $\tau \omega_c \gg 1$. This implies small collision broadening of the Landau levels. Then, in order to smear out the quantum Shubnikov–de Haas oscillations, the temperature must be sufficiently high, so that the sum over Landau quantum numbers in Eq. (2.12) can be replaced by an energy integration over $E_n = \hbar \omega_c (n + 1/2)$, and it must be sufficiently low, that this integration yields only contributions from the neighborhood of the Fermi energy. This leads to the condition[9,4] $T_c < T < T_a$ with $k_B T_c = \hbar \omega_c / 2\pi^2$ and $T_a = (\pi k_F / K) T_c$, and implies that $\hbar \omega_c \ll E_F$ so that many Landau levels are occupied. For $n \gg 1$ the asymptotic relations

$$F_n(u) \approx J_0(KR_n), \quad G_n(u) \approx J_1(KR_n) R_n / (Kl^2) \quad (2.13)$$

hold with $R_n = l\sqrt{2n+1}$. With $R_n = R_c = l^2 k_F$ valid at $E_n = E_F$, and a spin degeneracy factor 2, Eq. (2.12) agrees with Eq. (2.11) for $\mu = \nu = y$, $V_{\vec{q}} = V_0/2$ and $\omega_{\vec{q}} = \omega_m/2$ if $\vec{q} = (K,0,0)$ or $(-K,0,0)$ and $V_{\vec{q}} = \hbar \omega_{\vec{q}} = 0$ otherwise. The case $V(x) = V_0 \cos Kx$ and $B_m(x) = B_m \sin Kx$, where the phase of the magnetic modulation is shifted by $\pi/2$ with respect to the electric one, has also been considered in Ref. 9, and is called ''out-of-phase'' modulation. For this case, Eq. (2.12) was obtained with $W_n(u) = \{[V_0 F_n(u)]^2 + [\hbar \omega_m G_n(u)]^2\}^{1/2}$, which reduces in the quasiclassical limit also to Eq. (2.11), but with $\omega_{\vec{q}} = \omega_m/2i = -\omega_{-\vec{q}}$ for $\vec{q} = (K,0,0)$. In Sec. III it will become clear how such phase shifts can be realized experimentally.

D. Correction to resistivity

From the comparison with the quantum mechanical calculation, we see that our quasiclassical calculation can be valid only in the temperature window $T_c < T < T_a$. Further limitations are implied by taking the average of the modulation effects over unperturbed cyclotron orbits, which, incidentally, corresponds to the neglect of Landau level mixing in the quantum calculations.[9,4] It implies $\tau \omega_c \gg 1$ and that the correction (2.11) to the Drude conductivity can be correct only to lowest order in the modulation strengths. Thus we may readily transform Eq. (2.11) into the corresponding lowest-order correction to the Drude *resistivity* tensor. To leading order in $(\tau \omega_c)^{-1}$ we obtain

$$\Delta \rho_{\mu\nu} = \rho_0 \frac{\lambda_f^2}{2 E_F^2} \sum_{\vec{q} \neq 0} q_\mu q_\nu |\mathscr{S}_{\vec{q}}|^2, \quad (2.14)$$

where $\rho_0 = m/(e^2 n_{\text{el}} \tau)$ is the Drude resistivity and $n_{\text{el}} = k_F^2/(2\pi)$ the density of the homogeneous 2DEG with the mean free path $\lambda_f = \tau \hbar k_F / m$.[16] For sufficiently small values of the homogeneous magnetic field, actually for $qR_c \equiv q\lambda_f / \tau \omega_c \gtrsim 2$, the Bessel functions in Eq. (2.9) may be replaced by their large-argument asymptotic expansions, so that

$$\mathscr{S}_{\vec{q}} \approx \left(\frac{2}{\pi q R_c} \right)^{1/2} \left[\sigma_{B_0} V_{\vec{q}} \cos\left(q R_c - \frac{\pi}{4} \right) \right.$$
$$\left. + \frac{k_F}{q} \hbar \omega_{\vec{q}} \sin\left(q R_c - \frac{\pi}{4} \right) \right]. \quad (2.15)$$

''Flat-band'' conditions with $\mathscr{S}_{\vec{q}} = 0$, at which the $\vec{q}$th Fourier component of the modulation yields no contribution to $\Delta \rho_{\mu\nu}$, can occur only if $V_{\vec{q}}$ and $\hbar \omega_{\vec{q}}$ have the same complex phase, as, e.g., for pure cosine modulations. It is interesting to note that the magnetic analog of the dimensionless amplitude factor $V_{\vec{q}}/E_F$ of the electric modulation is the ratio of two lengths, $(k_F/q) \hbar \omega_{\vec{q}} / E_F = 2/(q R_{\vec{q}})$. Here $2\pi/q$ is the wavelength and $R_{\vec{q}} = v_F / \omega_{\vec{q}}$ the ''cyclotron radius'' in the magnetic modulation field, which, in contrast to the energy quantum $\hbar \omega_{\vec{q}}$, both are meaningful in the classical limit.

When the modulations become too strong as compared to $\hbar \omega_c$, the classical orbits may be completely different from cyclotron orbits. For a 1D modulation, channeling along po-

tential minima may occur for the electrostatic case[17] and along ''snake orbits'' in the magnetic case,[18] so that Eq. (2.14) is not applicable in the limit $B_0 \to 0$. For a strong 2D modulation (''antidot lattice'') reflection from antidots may lead to chaotic orbits. But even for a weak 2D modulation quantum effects may render Eq. (2.14) useless. Bragg reflections in the 2D superlattice may lead to a complicated internal subband structure of the Landau levels with weak dispersion and large gaps (Hofstadter spectrum), so that the group velocities, i.e., the quantum analog of the drift velocities (2.8), become very small and the band conductivity is dramatically suppressed.[4] The importance of these quantum effects depends on the relative magnitude of collision broadening and modulation broadening of the Landau levels and on their separation $\hbar \omega_c$, and is hardly predictable within the quasiclassical approach.

III. EXAMPLES

A. Modulation model

We now want to adapt Eq. (2.14) to typical experimental situations met in a $Al_{1-x}Ga_xAs$-GaAs heterostructure with lithographically patterned surface. A periodic array of one- or zero-dimensional ferromagnetic structures on the surface creates a periodic magnetic field in the plane of the 2DEG located at some distance below the surface. Strong modulation effects have been observed for one-dimensional lattices of parallel metal (Dy) strips[11] and for square lattices of Dy posts.[19]

In order to model the magnetic stray fields of such structures, we take the surface as the x-y plane and the semiconductor in the half space $z < 0$, with the two-dimensional electron gas located in a plane $z = -D < 0$. For a rectangular lattice we assume at the lattice sites $\vec{R} = (n_x a_x, n_y a_y, 0)$, for all integer values n_x and n_y, replica of a cylinder at the origin, with height h, $0 < z < h$, and either a circular basis of radius r_0, $x^2 + y^2 < r_0^2$, or a rectangular basis with $|x| < b_x/2$ and $|y| < b_y/2$. For a one-dimensional modulation we use metal strips with rectangular cross sections, located at $0 < z < h$, $|x - n_x a_x| < b_x/2$ (for all integers n_x) and translational invariant in the y direction. For the sake of simplicity, we assume that these metal structures are homogeneously magnetized, with a magnetization $\vec{M}(\vec{r}, z) = \vec{M}_0$ inside and $\vec{M}(\vec{r}, z) = 0$ outside the metal. We take $\vec{m}$ to represent the magnetic moment of a unit cell. Then, the ''magnetic charge density'' $-\vec{\nabla} \cdot \vec{M}$ is concentrated on the boundary faces of the metal structures, and acts as the source of the static magnetic field $\vec{H}(\vec{r}, z) = \vec{B} - 4\pi \vec{M} = -\vec{\nabla} \phi$, where the scalar potential ϕ satisfies Poisson's equation in the form

$$\Delta \phi = 4\pi \vec{\nabla} \cdot \vec{M}. \quad (3.1)$$

The solution of Eq. (3.1) with the standard boundary conditions of Maxwell's theory is a straightforward problem of magnetostatic. Defining two-dimensional Fourier expansions as in Eq. (2.2), we obtain for the scalar potential in the half spaces $z < 0$ and $z > h$, and for $\vec{q} \neq 0$,

$$\phi_{\vec{q}}(z) = \frac{2\pi}{a_x a_y} \left[\frac{\vec{q} \cdot \vec{m}_\parallel}{iq} + m_z \operatorname{sgn} z \right] F_{\vec{q}} e^{-q|z - h/2|}, \quad (3.2)$$

with $\vec{m}_\parallel = (m_x, m_y, 0)$ and $F_{\vec{q}}$ the form factor, which depends on the shape of the micromagnets on top of the semiconductor surface. For $\vec{q} = 0$, a linear function of z solves Eq. (3.1) in the half spaces $z < 0$ and $z > h$, corresponding to a homogeneous magnetic field in z direction. Since our magnets in the layer $0 < z < h$ cannot produce such homogeneous fields, we must put $\phi_{\vec{q}=0}(z) \equiv 0$. In these half spaces, the magnetic flux density is given by $\vec{B}(\vec{r}, z) = -\vec{\nabla} \phi(\vec{r}, z)$. Considering a strictly two-dimensional model for the electron gas, we neglect the x and y components of the magnetic flux density and calculate the magnetic modulation field $B_m(\vec{r}) = B_z(\vec{r}, z = -D)$ from the Fourier coefficients

$$B_{\vec{q}}(z) = \frac{2\pi}{a_x a_y} [i\vec{q} \cdot \vec{m}_\parallel + qm_z] F_{\vec{q}} e^{-q|z - h/2|}. \quad (3.3)$$

If one concentrates the magnetization of the metallic posts in their centers, i.e., assumes ideal magnetic dipoles, one can immediately calculate the Fourier coefficients of the lattice sum of the magnetic dipole fields to obtain Eq. (3.3) with $F_{\vec{q}} \equiv 1$. For the magnetized circular cylinders one obtains

$$F_{\vec{q}} = \frac{2J_1(qr_0)}{qr_0} \frac{\sinh(qh/2)}{qh/2}, \quad (3.4)$$

with J_1 the Bessel function, and for cylinders with rectangular basis[20]

$$F_{\vec{q}} = \frac{\sin(q_x b_x/2)}{q_x b_x/2} \frac{\sin(q_y b_y/2)}{q_y b_y/2} \frac{\sinh(qh/2)}{qh/2}. \quad (3.5)$$

If the cylinders merge in the y direction, i.e., for $b_y = a_y$, Eq. (3.5) reduces to the form factor for the 1D strip lattice,

$$F_{\vec{q}} = \delta_{q_y, 0} \frac{\sin(q_x b_x/2)}{q_x b_x/2} \frac{\sinh(qh/2)}{qh/2}. \quad (3.6)$$

We want to emphasize some features of these results. (i) The spatial orientation of the magnetization of the micromagnets determines the complex phases of the Fourier coefficients. A magnetization in the z direction ($\vec{m}_\parallel = 0$) leads to real Fourier coefficients, that is, to a pure cosine expansion of the modulation magnetic field, whereas a magnetization parallel to the plane of the 2DEG ($m_z = 0$) leads to purely imaginary coefficients, i.e., a sine expansion. (ii) For the strip lattice only the magnetization perpendicular to the strip axes is relevant. A magnetization in the y direction has no effect. A magnetization with the direction of $\vec{m} = m_0(\sin\theta, 0, \cos\theta)$ results in a complex phase factor $\exp(i\theta)$. (iii) For our idealized periodic model without lateral confinement, the average of the modulation field over a unit cell vanishes in each plane of constant z, and the amplitude decreases exponentially with the distance of that plane from the surface at $z = 0$. Since with increasing distance the contributions from the individual micromagnets decrease only with an inverse power law, the field contributions of more and more micromagnets must interfere destructively in order to produce the exponential decrease. For a real laterally confined system this implies that finite-size effects become more important with increasing distance from the surface. In any plane $z = -D$ the average modulation field produced by a finite array of micro-

magnets on the surface must still vanish, as the average field of a single dipole on the surface does. But if one calculates the average only over a part of the plane, say the area below the finite array of micromagnets (i.e., essentially over the ''sample''), the cancellation due to destructive interference will in general not be complete. Especially the average taken in a *unit cell* of a *finite* array will no longer vanish.

The array of micromagnets attached to the surface of the semiconductor heterostructure not only allows us to apply a magnetic modulation field to the 2DEG, it also is the source of an effective electric modulation. The reason for this is the difference in the thermal expansion coefficients of the metal-lic magnets and the semiconductor, which results, at the low temperatures of the experiments, in a stress-induced bending of the conduction band edge.

Theoretical as well as experimental investigations have shown[13,14] that the stress-induced potential energy under a strip centered at $x=0$ has a central peak and two side ex-trema of opposite sign, similar to the second derivative of a Gaussian, $V(x) = -V_0\lambda^2[d^2\exp(-x^2/\lambda^2)/dx^2]$. To simulate stress effects in the 1D modulation case, we repeat this an-satz for all strips and obtain the Fourier coefficients

$$V_{q_x} = V_0\sqrt{\pi}(\lambda/a_x)(\lambda q_x)^2 e^{-(\lambda q_x)^2/4}e^{-|zq_x|}, \quad (3.7)$$

where we have introduced the required exponential z depen-dence by hand. To get the potential close to the form ob-tained in Ref. 13, we choose $\lambda = b_x/\sqrt{6}$.

To simulate the stress-induced potential below a circular cylinder we choose the rotational invariant second derivative of a Gaussian, i.e., $V(\vec{r}) = -V_0\lambda^2\Delta\exp(-r^2/\lambda^2)$. On a rect-angular lattice this leads to the Fourier coefficients

$$V_{\vec{q}} = V_0(\pi\lambda^2/a_x a_y)(\lambda q)^2 e^{-(\lambda q)^2/4}e^{-|zq|}, \quad (3.8)$$

where we take $\lambda = \rho/\sqrt{2}$.

B. One-dimensional modulation

We first consider the simplest description of one-dimensional lateral superlattices in terms of purely harmonic modulation fields, i.e., we take

$$V(x) = V_0\cos(qx), \quad B_m(x) = \mathrm{Re}[B_m^0 e^{iqx}], \quad (3.9)$$

with $q=2\pi/a$ and B_m^0 either real, for a cosine, or imaginary, for a sine modulation. The strip modulation discussed above reduces to this simple form if the distance D between the 2DEG and the surface becomes comparable with the period a or larger. According to Eq. (2.14) only $\Delta\rho_{xx}$ is different from zero, whereas the other tensor components of the resis-tance are not changed by the modulation. In Fig. 1 we show the resulting $\Delta\rho_{xx}$ in two different regimes of the applied homogeneous magnetic field B_0. Since a common amplitude factor in the electric and the magnetic modulation does not change the shape of the magnetoresistance curves, we write $V_0 = \gamma E_F\varepsilon$ and $(k_F/q)\hbar\omega_m^0 = \gamma E_F\mu$, with $\omega_m^0 = eB_m^0/mc$, and divide the resistance correction by $(q\lambda_f\gamma)^2/2$. Note that in the lower panel of Fig. 1 as well as in all the following magnetoresistance plots the magnetic field scale starts at a finite value of $a/2R_c$ and not at $a/2R_c=0$. We suppress the
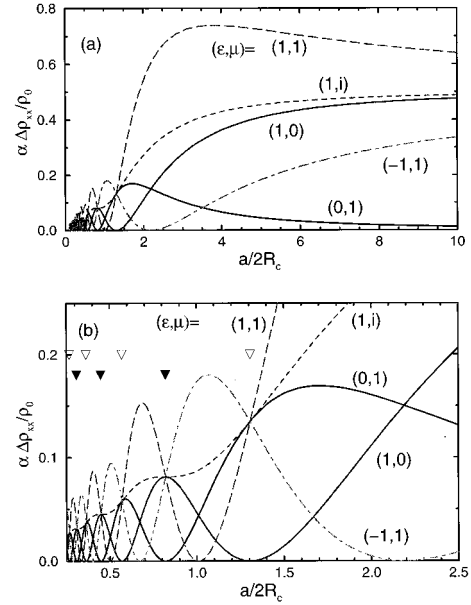

FIG. 1. Magnetoresistance vs scaled magnetic field for one-dimensional harmonic electric and magnetic modulations, $V(x) = V_0\cos(qx)$ and $B_m(x) = \mathrm{Re}[B_m^0\exp(iqx)]$, respectively, with $V_0 = \gamma E_F\varepsilon$ and $(k_F/q)\hbar\omega_m^0 = \gamma E_F\mu$, and the scaling factor $\alpha = 2/(\gamma q\lambda_f)^2$. The solid curves labeled $(\varepsilon,\mu)=(1,0)$ and $(0,1)$ refer to purely electric and purely magnetic modulations, respec-tively. The long-dashed lines labeled $(1,1)$ refer to in-phase cosine modulations, the dash-dotted lines labeled $(-1,1)$ to cosine modu-lations with phase difference π, and the short-dashed lines labeled $(1,i)$ to modulations with phase difference $\pi/2$. In (b) the results of (a) are shown in greater detail, and the electric and magnetic flat-band conditions are indicated by open and filled triangles, respec-tively.

region of small values of the applied magnetic field B_0, since there our calculation scheme is not applicable.

In Fig. 1 the solid curves labeled $(\varepsilon,\mu)=(1,0)$ and $(0,1)$ give the resistance change due to only electric and only mag-netic modulation, respectively. According to the values of the Bessel functions for zero argument, the magnetoresis-tance due to the magnetic modulation approaches zero for large B_0 ($\Delta\rho\propto1/B_0^2$), whereas that due to the electric modu-lation saturates, such as the curve $(1,0)$ in Fig. 1(a), which approaches the value 0.5. In the case of only electric modu-lation, $\Delta\rho$ vanishes at the ''electrical flat-band conditions'' $a/2R_c=1.306, 0.569, \ldots$, indicated by the open triangles in Fig. 1(b). They are determined by the zeroes of the Bessel function J_0 and are, according to Eq. (2.15), well approxi-mated by

$$2R_c \approx a(\lambda_e - 1/4), \quad \lambda_e = 1,2,\ldots. \quad (3.10)$$

For purely magnetic modulation, $\Delta\rho$ vanishes at the mag-netic flat-band conditions $a/2R_c=0.820, 0.448, \ldots$, indi-cated by the filled triangles. They are determined by the ze-roes of J_1 and are, according to Eq. (2.15), accurately approximated by

$$2R_c \approx a(\lambda_m + 1/4), \quad \lambda_m = 1,2,\ldots. \quad (3.11)$$

For λ_e and λ_m larger than 1, Eqs. (3.10) and (3.11) approxi-mate the correct values with an error of less than 1%.

The long-dashed curve, labeled (1,1), refers to the case where electric and magnetic modulation are in phase. For B_0 larger than the last electric flat-band condition ($a/2R_c > 4/3$), all contributions to Eq. (2.9) are positive, and, for very large B_0 values, this magnetoresistance curve approaches the curve for pure electric modulation from above. For B_0 values between the last electric and the last magnetic flat-band condition ($4/3 > a/2R_c > 4/5$), the Bessel function J_0 in Eq. (2.9) assumes negative values while J_1 is still positive. Here the effects of electric and magnetic modulation interfere destructively and cancel each other at that value of B_0 where the magnetoresistance due to a purely electric modulation equals that of a purely magnetic modulation. If we turn on the magnetic modulation continuously, so that μ increases from 0 to 1, the long-dashed curve evolves from that with pure electric modulation in such a manner that the zeroes shift from the electric flat-band conditions towards the corresponding magnetic flat-band conditions with $\lambda_m = \lambda_e$, i.e., to smaller values of B_0.

If we keep the modulations fixed, invert the direction of the applied homogeneous field ($B_0 \rightarrow -B_0$), and plot the magnetoresistance versus $|B_0|$, we obtain the dash-dotted curves labeled ($-1,1$). The same result is obtained if we keep B_0 positive and change the relative sign between V_0 and B_m^0, i.e., superpose electric and magnetic cosine modulations with a phase difference of π. Now the B_0 regions of constructive and destructive interference are interchanged. For large B_0 values the dash-dotted curve approaches the curve for purely electric modulation from below. If we turn on the magnetic modulation gradually, the dash-dotted curve evolves from that for purely electric modulation in such a manner that the zeroes shift to larger B_0 values, i.e., from electric flat-band condition with a certain λ_e to the magnetic flat-band condition with $\lambda_m = \lambda_e - 1$, for $\lambda_e > 1$. Since $J_1(0) = 0$, we may extend this statement to the case $\lambda_e = 1$, if we define the magnetic flat-band condition for $\lambda_m = 0$ as the limit $2R_c/a \rightarrow 0$. Equation (3.11) corresponds to the large-argument expansion of the Bessel functions, see Eq. (2.15), which is not applicable for $2R_c/a < 3/4$.

This asymmetry under inversion of the direction of the applied homogeneous magnetic field has been observed in experiment,[11] and it has been exploited to determine the sign of the stress-induced electrostatic potential from the known direction of the magnetic modulation field.

The short-dashed curves in Fig. 1 are obtained for $(\varepsilon, \mu) = (1, i)$, i.e., an electrical cosine and a magnetic sine modulation (phase difference $\pi/2$). In this case the contributions of the purely electric and the purely magnetic modulation simply add, without any interference. In this case there are no zeroes of the magnetoresistance or corresponding flat bands in the quantum mechanical description.[9] This is also in agreement with recent experiments in which the Dy strips were magnetized in the direction perpendicular to their axes and parallel to the plane of the 2DEG.[15]

The harmonic approximation of the magnetic modulation field considered in Fig. 1 is an oversimplification and does not hold in the existing experiments, where the distance between the 2DEG and the surface is only 10–20 % of the period a of the strip lattice. Figure 2 gives an impression of the stray field generated by a strip lattice as a function of the strip height for a given strip width $b_x = 0.6a$. For a homoge-
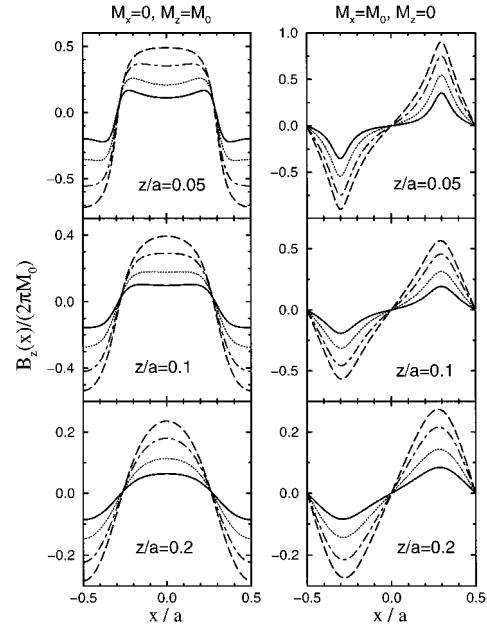

FIG. 2. Magnetic modulation field $B_z(x)$ produced by a lattice of period a in the x direction of strips, which have the width $b_x = 0.6a$ and are homogeneous in the y direction. A homogeneous magnetization of modulus M_0 is taken in the z direction perpendicular to the surface (left panels), or in the x direction parallel to the surface (right panels). The strip heights h are chosen as $h/a = 0.05$ (solid lines), 0.1 (dotted lines), 0.2 (dashed-dotted lines), and 0.4 (dashed lines). The x dependence of B_z is shown in planes at distances $z = 0.05a$, $0.1a$, and $0.2a$ (from top to bottom) below the surface plane at $z = 0$.

neous magnetization of a given value M_0, the amplitude of the modulation field in any plane below the surface increases with increasing height of the strips, but the x dependence becomes smoother, since the added magnetized material has a larger distance from this plane and thus contributes predominantly to the lowest harmonics.

A more realistic situation is considered in Fig. 3. The magnetic field is calculated according to Eqs. (3.3) and (3.6) for a lattice with period $a_x = a$ of strips which are homogeneous in the y direction. The stress-induced electrostatic potential is modeled by Eq. (3.7). In the upper panels the homogeneous magnetization of the strips is assumed in the x direction, i.e., parallel to the plane of the 2DEG and perpendicular to the axes of the strips. In the lower panels it is taken in the z direction, perpendicular to the strips and to the plane of the 2DEG. As is seen in the left panels in Fig. 3, the fields contain higher harmonics. These have as consequence that the magnetoresistance curves in the lower right panel do not go down to zero at their minima. The dash-dotted line, presenting the result for purely electrostatic modulation, has minima at slightly lower B_0 values as those given by the ideal flat-band condition (3.10), e.g., near $a/2R_c = 1.22$ instead of $a/2R_c = 1.31$. As the amount of magnetic modulation is increased ($\mu = 0.5$, 1.0, 1.25), the minima shift towards the magnetic flat-band conditions with $\lambda_m = \lambda_e$ as discussed above. At the magnetic flat-band conditions all the curves with the same amount of electric modulation ($\varepsilon = 1$) intersect each other at the same value for the magnetoresistance. This indicates that the higher harmonics of the mag-
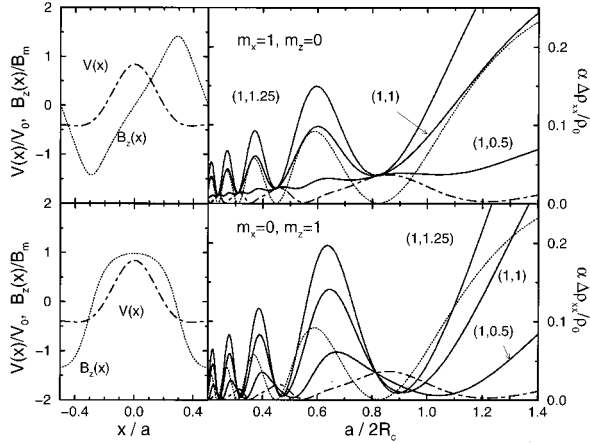
FIG. 3. Modulation fields (left panels) and resulting magnetoresistance (right panels) for a one-dimensional lattice (period $a_x=a$) of magnetized strips of width $b_x=0.6a$ and height $h=0.4a$, and a two-dimensional electron gas at $z=-0.1a$. The fields are given by Eq. (3.7) with $V_0=\gamma E_F \varepsilon$ and by Eqs. (3.3), (3.6) with $B_m=2\pi|\vec{m}|/(a_x^2 a_y)$. The magnetic moment $\vec{m}$ is taken in the x direction in the upper panels and in the z direction in the lower panels. Its magnitude is chosen so that $(ak_F/2\pi)\hbar eB_m/mc=\gamma E_F \mu$. In the right panels, the dash-dotted lines refer to purely electric modulation, i.e., $(\varepsilon,\mu)=(1,0)$, the dotted lines to purely magnetic modulation, $(\varepsilon,\mu)=(0,1)$, and the solid lines to a mixed modulation with the indicated (ε,μ) values. The scaling factor is $\alpha=2a^2/(2\pi\gamma\lambda_f)^2$.

netic modulation are less effective than those of the electric modulation, as is to be expected from Eq. (2.9). In contrast to the resistance curves in the lower panel, those in the upper panel do not *intersect* each other at the magnetic flat-band conditions, although they all assume there the same values, namely, those for the purely electric modulation. This characteristic difference between the two directions of magnetization is a direct consequence of the different complex phases of the Fourier coefficients in both cases, and has recently been observed in experiments.[15]

C. Square lattice of magnetized cylinders

In samples with a two-dimensional periodic array of micromagnets, an in-plane component of the magnetization leads to an anisotropic magnetoresistance tensor. In contrast to the case of 1D strip arrays, where the anisotropy is trivial (only $\Delta\rho_{xx}\neq0$), now in general both $\Delta\rho_{xx}$ and $\Delta\rho_{yy}$ are nonzero and different from each other. Thus, in addition to the size and the form of the micromagnets, and to the relative magnitude of stress-induced electrostatic and of magnetic modulations, the *orientation* of the magnetization will influence the magnetoresistance curves. Among the huge number of possible experimental situations, we will choose only a few typical examples, with parameters that are accessible to the experiment.

We consider a square lattice, with period a (say, $a=500$ nm), of circular cylinders with radius $\rho=0.25a$ and height $h=0.4a$ on the sample surface in the plane $z=0$, and a 2DEG in the plane $z=-0.2a$ below the surface. The stress-induced potential is modeled by Eq. (3.8) with $V_0=\gamma E_F \varepsilon$ and kept fixed in the following. It is visualized in the upper
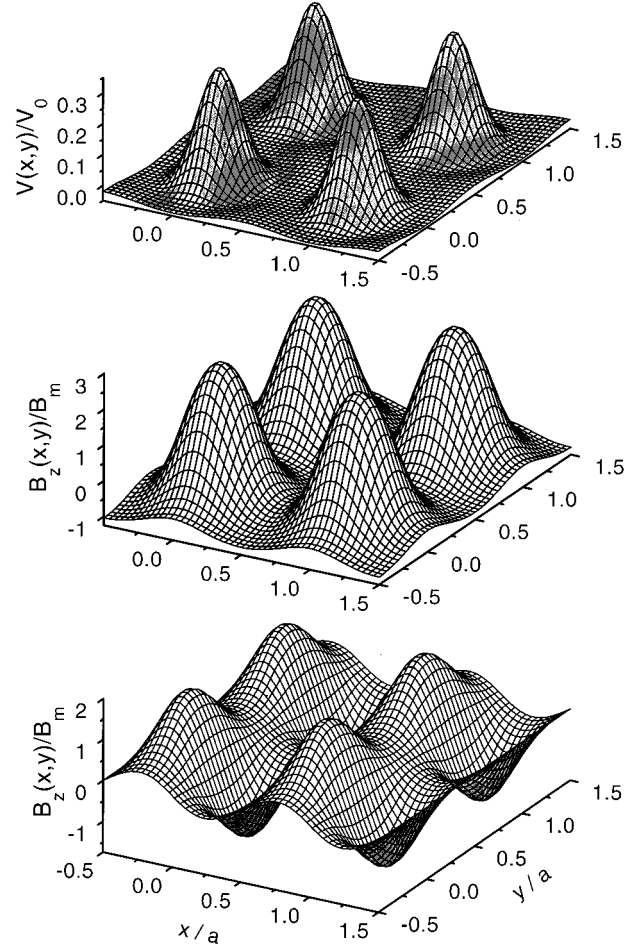

FIG. 4. Modulation fields in the plane of the two-dimensional electron system due to a square lattice of homogeneously magnetized circular cylinders on the sample surface. Top: stress-induced electrostatic potential energy in the model of Eq. (3.8). Middle and bottom: normal component of the periodic magnetic field due to a magnetization of the cylinders in the z direction perpendicular (middle) and in the x direction parallel (bottom) to the plane of the 2DEG. Sample parameters are given in the text.

part of Fig. 4. The magnetic modulation is calculated from Eqs. (3.3) and (3.4), with $a_x=a_y=a$ and $B_m=2\pi|\vec{m}|/a^3$.

We first take the magnetization vector in the x-z plane, $\vec{m}=|\vec{m}|(\sin\theta,0,\cos\theta)$. The resulting magnetic modulation is visualized in the middle part of Fig. 4 for a magnetization in the z direction ($\theta=0$), perpendicular to the plane of the 2DEG, and in the lower part of Fig. 4 for a magnetization in the x direction ($\theta=\pi/2$). It is seen that, at the given distance between the 2DEG and the surface, the modulation fields still have a lot of harmonic content and are not simply sinusoidal. Whereas the modulation field for $\theta=0$ is invariant under rotations along the z axis at multiples of $\pi/2$, the modulated magnetic field $B_z(\vec{r},z=-D)$ for $\theta=\pi/2$ is seen to be very anisotropic, without rotational symmetry. Its maximum variation along a line in the y direction is at most half as large as the maximum variation along the lines in the x direction corresponding to constant, integer values of y/a. The modulation in the y direction is only due to higher harmonics with periods shorter than a, since according to

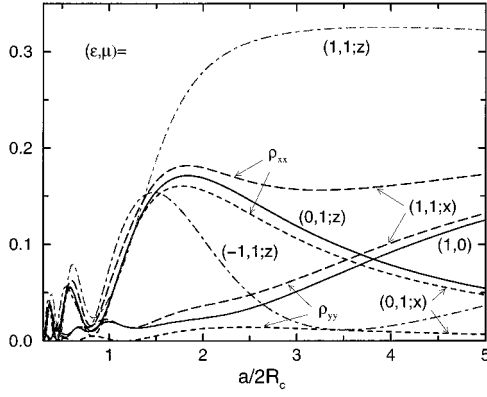FIG. 5. Magnetoresistance for simple superpositions of the modulation fields depicted in Fig. 4. Solid lines for pure electric, $(1,0)$, and pure magnetic, $(0,1;z)$, modulation due to magnetization in the z direction, dash-dotted lines for constructive, $(1,1;z)$, and destructive, $(-1,1;z)$, superpositions of these modulations. These four lines represent isotropic situations with $\Delta\rho_{yy}=\Delta\rho_{xx}$. The dashed lines are for magnetization in the x direction with, $(1,1;x)$, and without, $(0,1;x)$, superposition of the electric modulation. Scaling parameter α as in Fig. 3.

Eq. (3.3) only Fourier coefficients $B_{\vec{q}}$ with $q_x \neq 0$ are nonzero. At larger distances, where only the fundamental periodicities survive, the position dependence of this modulation field reduces to $\propto \sin(2\pi x/a)$, whereas the position dependence of the electrostatic potential and that of the modulation due to a magnetization in the z direction reduce to the form $\propto [\cos(2\pi x/a)+\cos(2\pi y/a)]$.

In Fig. 5 we show the magnetoresistance curves calculated for simple combinations of these modulation fields. We describe the amplitude of the magnetic modulation in terms of μ, defined by $(2\pi k_F/a)\hbar e B_m/mc = \gamma E_F \mu$, and scale the factor γ^2 out of the resistance results as before. The solid curve labeled $(1,0)$ presents the result for the stress modulation only. Due to the higher harmonics (see upper panel of Fig. 4) only a shallow minimum appears near the electric flat-band condition $a/2R_c \approx 1.3$, and an additional minimum occurs near the magnetic flat-band condition $a/2R_c \approx 0.8$. This minimum is due to the harmonics with wave vectors $\vec{q}=(\pm 2,\pm 2)\pi/a$, which yield zero contribution at the flat-band condition $qR_c = \pi(\lambda - 1/4)$, with $\lambda = 2$ and $q = \sqrt{2}(2\pi/a)$. The solid line labeled $(0,1;z)$ refers to purely magnetic modulation due to magnetization in the z direction. The finite values of the magnetoresistance at the magnetic flat-band condition $a/2R_c \approx 0.8$ indicates higher harmonics. The dash-dotted lines labeled $(1,1;z)$ and $(-1,1;z)$ refer to a superposition of these two fields with equal $[\sigma_{B_0}=+1$ in Eq. (2.9)] and opposite $(\sigma_{B_0}=-1)$ phases, respectively. It is easily seen from Eqs. (3.3) and (3.4) that, for magnetization only in the z direction, $B_{\vec{q}}$ and therefore $|\mathscr{S}_{\vec{q}}|$ in Eq. (2.14) depend only on $|\vec{q}|$. As a consequence, $\Delta\rho_{xx}=\Delta\rho_{yy}$ and $\Delta\rho_{xy}=\Delta\rho_{yx}=0$, i.e., the tensor $\Delta\rho$ is isotropic.

The magnetoresistance components for a purely magnetic modulation due to a magnetization in the x direction are indicated by the short-dashed lines in Fig. 5, labeled $(0,1;x)$. The strong anisotropy is obvious: $\Delta\rho_{xx}$ is rather similar to the solid line labeled $(0,1;z)$ [the difference being only due to higher harmonics, see Eqs. (3.3) and (3.4)] and
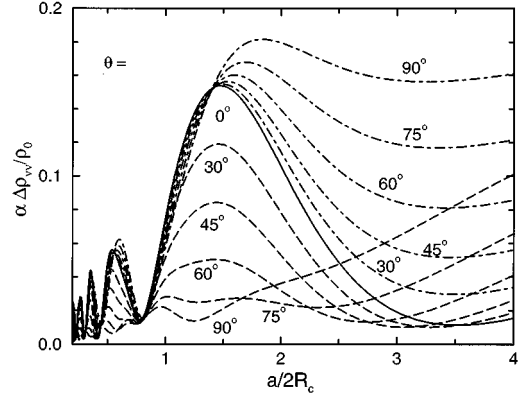

FIG. 6. Magnetoresistance curves for different tilt angles of the magnetization between the z direction ($\theta = 0°$) and the x direction ($\theta = 90°$). The upper curves (dashed-dotted) show $\Delta\rho_{xx}$, the lower ones (dashed) show $\Delta\rho_{yy}$; α as in Fig. 3.

has pronounced minima at the magnetic flat-band conditions, whereas $\Delta\rho_{yy}$ assumes much smaller values (being nonzero only due to higher harmonics) and has even a maximum at the magnetic flat-band condition $a/2R_c \approx 0.8$. The long-dashed lines labeled $(1,1;x)$ indicate the result obtained for a superposition of this magnetic modulation with the stress-induced electric modulation. Here the contributions to the magnetoresistance due to magnetic and electric modulation simply add (the sign of σ_{B_0} is irrelevant since the Fourier coefficients describing the magnetic modulation are purely imaginary).

Experimentally it seems impossible to measure a magnetoresistance curve for a magnetic modulation due to a magnetization which is strictly parallel to the 2DEG, since the applied homogeneous field B_0 will always produce a z component of the magnetization. It is, therefore, of interest to follow the change of the magnetoresistance as the magnetization is tilted with respect to the surface normal. Such a variation is shown in Fig. 6. We take $\vec{m}=|\vec{m}|(\sin\theta,0,\cos\theta)$ and, with our usual convention for the amplitudes of the modulation field, $(\varepsilon,\mu)=(-1,1)$, so that we have a destructive interference between the electric modulation and the magnetic modulation due to the z component of $\vec{m}$ for $a/2R_c > 1.31$. The solid line in Fig. 6 indicates $\Delta\rho_{xx}=\Delta\rho_{yy}$ for $\theta = 0°$. The dash-dotted lines refer to $\theta = 30°$, the dotted lines to $\theta = 45°$, etc. The upper lines represent $\Delta\rho_{xx}$, which for large values of B_0 ($a/2R_c > 1.5$) increases with increasing tilt angle θ. The lower lines indicate $\Delta\rho_{yy}$, which in the region of the maximum close to $a/2R_c = 1.5$ decreases with increasing θ.

In all situations we have considered so far, the symmetry $|\mathscr{S}_{(-q_x,q_y)}|=|\mathscr{S}_{(q_x,q_y)}|$, which follows from Eq. (3.3) for $m_y = 0$, leads with Eq. (2.14) to $\Delta\rho_{xy}=\Delta\rho_{yx}=0$. This is no longer true if the magnetization has finite x and y components, i.e., $m_x m_y \neq 0$. From Eqs. (3.3) and (2.14) we obtain

$$\Delta\rho_{xy}/\rho_0 = m_x m_y P \sum_{q_x,q_y>0} [q_x q_y F_{\vec{q}}(z) J_1(qR_c)]^2$$

$$(3.12)$$

with $F_{\vec{q}}(z)=F_{\vec{q}}\exp(-q|z-h/2|)$ and the prefactor $P=(4\pi\lambda_f\hbar e)^2/(E_F a_x a_y mc)^2$. Note that $\Delta\rho_{yx}=\Delta\rho_{xy}$, so
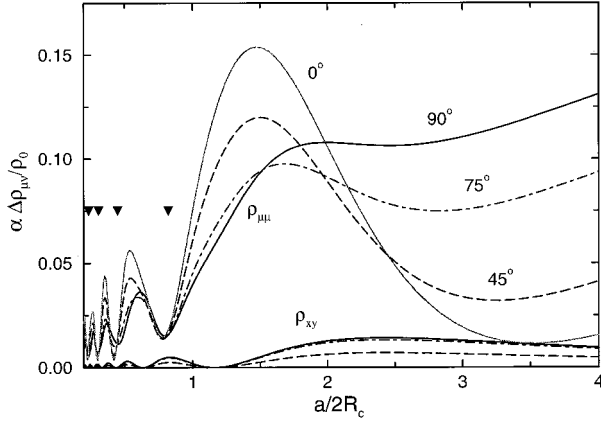
FIG. 7. Magnetoresistance curves for different tilt angles of the magnetization between the z direction ($\theta=0°$) and the direction $x=y$ in the x-y plane ($\theta=90°$). The upper curves show the diagonal contributions $\Delta\rho_{xx}=\Delta\rho_{yy}$, the lower ones the off-diagonal contributions $\Delta\rho_{xy}=\Delta\rho_{yx}$. Same line styles refer to equal tilt angles, $\Delta\rho_{xy}(0°)\equiv0$, α as in Fig. 3. The black triangles indicate the magnetic flat-band conditions as in Fig. 1.

that the tensor $\Delta\rho$ is real and symmetric and can be diagonalized by a rotation of the coordinate axes, and that only higher harmonics (with $q_x\neq0$ and $q_y\neq0$) contribute. It is also interesting to note that these off-diagonal contributions are independent of the z component of the magnetization and of the electric modulation. As a consequence, the plot of $\Delta\rho_{xy}$ versus the applied homogeneous magnetic field B_0 should only change its magnitude but not its shape if the relative strengths of magnetic and electric modulations are changed, in contrast to the plots of the diagonal contributions to $\Delta\rho$.

In Fig. 7 we present results for the symmetric case $m_x=m_y$ and different tilt angles θ with respect to the z axis, $\vec{m}=|\vec{m}|(\sin\theta,\sin\theta,\sqrt{2}\cos\theta)/\sqrt{2}$. For $\theta=0$ we obtain the previous isotropic result. For $\theta>0$ we still obtain $\Delta\rho_{xx}=\Delta\rho_{yy}$, since the modulation is symmetric with regard to the interchange of x and y. The main features of the results in Fig. 7 are not difficult to understand. At the magnetic flat-band conditions for the fundamental period ($a/2R_c = 0.82, 0.45, 0.31, \ldots$) all the curves for the diagonal magnetoresistance assume similar values, close to the value for pure electric modulation. This indicates that $\Delta\rho_{xx}$ is dominated by the fundamental period of the magnetic modulation. The minima of the $\Delta\rho_{xx}$ curves for $\theta=0°$ and 45° near $a/2R_c = 3.3$ and 0.4 are due to destructive interference between the electric modulation and the magnetic modulation as a result of the z component of the magnetization. The values at the minima are dominated by higher harmonics in the case of $\theta=0°$ and by contributions due to the in-plane component of the magnetization for $\theta=45°$. With increasing θ, the interference becomes less important and the minimum becomes less pronounced and shifts from $a/2R_c\approx 3.5$ for $\theta=0$ to $a/2R_c\approx 2.5$ for $\theta=90°$. At the same time $\Delta\rho_{xy}$ increases without any change of its shape from zero for $\theta=0°$ to its full value at $\theta=90°$, saturating rapidly for $\theta>60°$. The minima of $\Delta\rho_{xy}$ occur at the flat-band conditions for the harmonics with $|\vec{q}|=\sqrt{2}(2\pi/a)$ at $a/2R_c=1.16, 0.63$, etc.
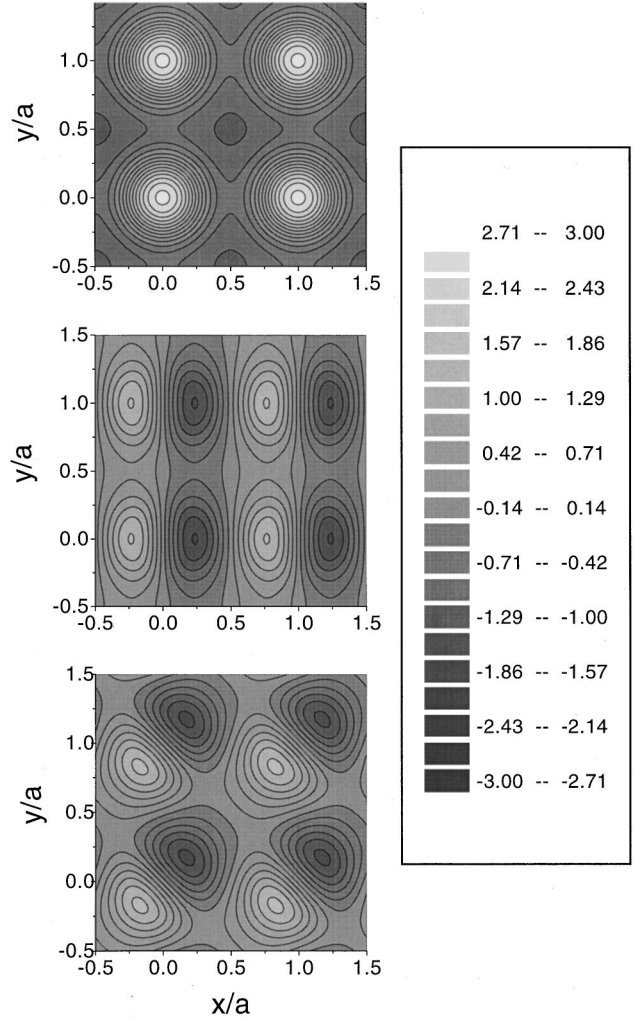

FIG. 8. Contour plots of the magnetic modulation field $B_z(x,y)/B_m$ for magnetization in the z direction (top), in the x direction (middle), and for $m_x=m_y$, $m_z=0$ (bottom). Sample parameters are the same as those in the lower panels of Fig. 4. The indicated gray step code is used in all plots.

The symmetry property $\Delta\rho_{xx}=\Delta\rho_{yy}$ does not mean that the resistance tensor is isotropic, since now $\Delta\rho_{yx}=\Delta\rho_{xy}\neq0$. Obviously this tensor can be diagonalized by a rotation of the x and y coordinate axes by $\pi/4$, with eigenvalue $\Delta\rho_{xx}+\Delta\rho_{xy}$ in the (1,1) direction and eigenvalue $\Delta\rho_{xx}-\Delta\rho_{xy}$ in the (1,−1) direction. This symmetry is easily understood from the contour plots in Fig. 8. These show the variation of the magnetic modulation field $B_m(x,y)$ for three high-symmetry directions of the magnetization. For $\vec{m}$ in the z direction, the pattern has the full square symmetry, and the $\Delta\rho$ tensor is isotropic. For $\vec{m}$ in the x direction, the pattern is symmetric under reflection at the x axis and antisymmetric under reflection at the y axis, but it has no rotational symmetry. As a result, the $\Delta\rho$ tensor is diagonal, but with $\Delta\rho_{xx}\neq\Delta\rho_{yy}$. Finally, for $\vec{m}$ in the direction (1,1,0), there is no mirror symmetry with respect to the x and y axes, and the $\Delta\rho$ tensor is not diagonal. However, the pattern is symmetrical under interchanging of x and y, so that the diagonal elements of the $\Delta\rho$ tensor are equal. This symmetry means that the pattern is symmetrical under reflection at the

diagonal through the origin with slope $+1$, while it is anti-symmetric under reflection at the diagonal through the origin with slope -1. With respect to the axes of reflection symmetry, the $\Delta\rho$ tensor becomes diagonal, but not isotropic.

We mention in passing that the symmetric off-diagonal components of the $\Delta\rho$ tensor, which are due to anisotropy, do contribute to dissipation, whereas the antisymmetric off-diagonal components of the Drude resistivity tensor, which describe the Hall effect, do not. Another aspect is that the form of the Drude resistivity tensor is invariant under rotation of the coordinate axes, while the $\Delta\rho$ tensor can be diagonalized by a suitable rotation.

IV. CONCLUSIONS

We have generalized the quasiclassical theory of Weiss oscillations in two-dimensional electron gases to the case of superlattices defined by a combination of weak electrostatic and magnetic fields of arbitrary shapes, but with the same lattice constants. We have adapted fields to the experimental situation, where periodic arrays of nanostructured ferromagnets are deposited on the surfaces of the samples. We have idealized the situation in so far as we have assumed simple geometric shapes and homogeneous magnetization of these micromagnets. In experiments, the magnetization will not be homogeneous, since the micromagnets are not of ellipsoidal shape, and it will depend in a nonlinear hysteretic manner on the applied homogeneous magnetic field and its history. Nevertheless, the calculated interference effects of magnetic and electric modulations are in encouraging agreement with typical features observed in recent experiments.[11,15] Especially, tilting the magnetization with respect to the surface normal provides a new degree of freedom for the investigation of Weiss oscillations and may be a promising route to test our understanding of these transport effects in detail.

We have also discussed the limitations of this simple but fertile approach. The restrictions to a temperature window and to relatively low values of the applied magnetic field B_0 — so that the Weiss oscillations are resolved but not the Shubnikov–de Haas oscillations — are obviously of a quantum mechanical nature. The restrictions to sufficiently large B_0 values and small modulation amplitudes occur already within the classical treatment, since here, for the perturbation of the cyclotron orbits to remain small, the forces exerted on the electrons by the modulation fields must be much smaller than the Lorentz force due to the homogeneous field B_0. In this context it is interesting to remark that the sum in Eq. (2.14) diverges for an electrostatic step potential,[6] since the Fourier coefficients in each direction decay only as $1/q_\mu$. Obviously the electric field of the step potential has δ-function singularities and the corresponding force is not small as compared with the Lorentz force. It can also be shown that, in a one-dimensional periodic step potential $V(x)$, always orbits exist which are confined to a single period in the x direction and are traversed nearly with the Fermi velocity in the y direction. These orbits cannot be approximated by drifting cyclotron orbits, and their contribution to the magnetoresistance cannot be calculated perturbatively with respect to $V(x)$. Any attempt to do so leads to diverging results.

In two-dimensional superlattices a quantum mechanical

subband structure of the Landau bands (Hofstadter spectrum) may reduce the group velocities considerably. A strong reduction of the band conductivity observed in high-mobility samples with a weak electric modulation has been attributed to this quantum interference effect.[4] Whether there is a need for such a quantum transport theory in the situations considered in the present work will become clear after a detailed comparison of future experiments with the predictions of the quasiclassical approach presented here.

APPENDIX A

In the presence of modulations, we define for each point $\vec{r}$ of the modified cyclotron orbit the guiding center as the center of the circle which has in $\vec{r}$ the same tangent and the same radius of curvature R as the modified orbit. In terms of the length s along the orbit, this circle of curvature at the point $\vec{r}=\vec{r}(s_0)$ is given by

$$\vec{r}(s)=\vec{r}+R[\sin\varphi\,\vec{t}+(1-\cos\varphi)\vec{n}], \tag{A1}$$

with $\varphi=(s-s_0)/R$, and with $\vec{t}=(d\vec{r}/ds)/\dot{s}$ and $\vec{n}=Rd\vec{t}/ds$ the unit tangent and the unit normal vectors of the orbit at point $\vec{r}$, respectively. With $\dot{s}=v=|\dot{\vec{r}}|$, $\vec{v}=v\vec{t}$, and $\dot{\vec{v}}=\dot{v}\vec{t}+(v^2/R)\vec{n}$, one obtains from Newton's equation (2.1) $\dot{v}=-(e/m)\vec{E}\cdot\vec{t}$ and

$$\frac{v^2}{R}\vec{n}=-\frac{e}{m}\left[\vec{t}\times(\vec{E}\times\vec{t})+\frac{v}{c}\vec{t}\times\vec{B}\right]. \tag{A2}$$

Assuming the modulation fields to be sufficiently small, we obtain $\vec{n}=\vec{e}_z\times\vec{v}/v$ and

$$R=v/[\omega_c+\omega_m+e\vec{v}\cdot(\vec{e}_z\times\vec{E})/(mv^2)], \tag{A3}$$

where $\omega_m(\vec{r})=eB_m(\vec{r})/mc$. Apparently the radius of curvature R deviates from the unperturbed cyclotron radius R_c by a small correction, which vanishes linearly with vanishing amplitudes of the modulation fields. According to Eq. (A1), the center of the circle of curvature through $\vec{r}$ is given by

$$\vec{r}_M=\vec{r}+R\vec{n}=\vec{r}+(\vec{e}_z\times\vec{v})/\omega_c+\delta^{(1)}\vec{r}_M, \tag{A4}$$

which deviates from Eq. (2.4) only by the term $\delta^{(1)}\vec{r}_M$, which is of first order in the modulation fields. We want to calculate the average of the guiding-center drift velocity only to first order in these fields. As we see from Eqs. (2.4) and (2.5), the leading terms on the right hand side of Eq. (A4) lead to a result which is of first order in these fields, so that the average can be taken over the unperturbed cyclotron orbits. To evaluate the contribution of the correction term $\delta^{(1)}\vec{r}_M$ with the same accuracy, we must calculate its time derivative from Eq. (2.1) but with the modulation fields ne-

glected, i.e., here we have to take the time derivatives of the unperturbed cyclotron motion. Taking then the average over a cyclotron orbit, i.e., the integral with respect to the angle φ in Eq. (2.3) between $-\pi$ and π, we obtain a zero result. This is because the time derivative of $\delta^{(1)}\vec{r}_M$ along this cyclotron orbit is just ω_c times its derivative with respect to the angle. Thus, to first order in the modulation fields, the correction term $\delta^{(1)}\vec{r}_M$ in Eq. (A4) does not contribute to the *average* drift velocity.

APPENDIX B

In this appendix we sketch the derivation of the conductivity formula (2.11) from the more familiar form in terms of the velocity-velocity correlation function. For a spatially inhomogeneous, degenerate electron gas, the average current density as the linear response to a homogeneous electric field can be calculated, within the relaxation time approximation of Boltzmann's equation, from Chambers' formula.[21] This yields the conductivity in the form of Einstein's relation $\sigma_{\mu\nu} = e^2 D(E_F) D_{\mu\nu}$, with $D(E_F) = n_{el}/E_F$ the density of states at the Fermi level and

$$D_{\mu\nu} = \int_0^\infty dt e^{-t/\tau} \langle v_\mu(t) v_\nu(0) \rangle_{\text{initial}} \qquad (B1)$$

the diffusion tensor. Here the velocity $\vec{v}(t)$ is taken along a specific trajectory of an electron with energy E_F, that is allowed by Newton's equation of motion and determined by initial position $\vec{r}(0)$ and velocity $\vec{v}(0)$ at time $t=0$, and the average is taken over all possible initial conditions for the motion along such trajectories. When the velocity along a given trajectory is a periodic function of time with period T, as, e.g., for the cyclotron motion in a homogeneous 2DEG or in a 2DEG with modulation in only one lateral direction, the time integral in Eq. (B1) reduces to

$$\int_0^\infty dt e^{-t/\tau} v_\mu(t) = \int_0^T dt \frac{e^{-t/\tau} v_\mu(t)}{1 - e^{-T/\tau}}. \qquad (B2)$$

When the period T is much shorter than the relaxation time, the right hand side of Eq. (B2) can be approximated, to leading order in the small parameter $T/\tau \ll 1$, by

$$\frac{\tau}{T} \int_0^T dt v_\mu(t) = \tau v_\mu^D, \qquad (B3)$$

where v_μ^D is a Cartesian component of the average (drift) velocity along the trajectory, and has the same value for all possible initial conditions leading to motion along this trajectory. Then it is convenient to perform the average over initial conditions in Eq. (B1) in two steps. First, one averages over all initial conditions which lead to the same trajectory, and then the average over all possible trajectories is taken. Thus, to leading order in $T/\tau \ll 1$, Eq. (B1) reduces to

$$D_{\mu\nu} = \tau \langle v_\mu^D v_\nu^D \rangle_{\text{orbits}}. \qquad (B4)$$

Note that this result is consistent with the Drude conductivity of the homogeneous 2DEG. For $B_0 = 0$, the velocity is a constant of motion, $v_\mu(t) = v_\mu^D$, and one obtains $D_{\mu\nu} = \frac{1}{2}\tau v_F^2 \delta_{\mu\nu}$. For $B_0 \neq 0$ one has $v_\mu^D = 0$, and, for $\omega_c \tau \gg 1$, nonzero contributions come only from higher orders in the small parameter $T/\tau = 2\pi/(\omega_c \tau)$.

It is also interesting to note that, for the derivation of Eq. (B4), we did not need an assumption about the amplitude of the modulations. For one-dimensional periodic electric and magnetic modulations the motion in an externally applied, homogeneous magnetic field B_0 is bounded in the direction of the modulation, and the velocity along any allowed trajectory is a periodic function of time. Thus, Eq. (2.4) is applicable for arbitrary modulation strengths, even if the orbits are rather different from the unperturbed cyclotron orbits in the absence of modulations. The only condition is that the period T be much shorter than τ. This condition will be violated for very small values of B_0, but may hold again for $B_0 = 0$. In the regime of the Weiss oscillations we assume the modulations to be so weak, that, within a period T, each trajectory remains close to an unperturbed cyclotron orbit, and that the average (drift) velocity can be calculated along the latter. Consequently the average over orbits reduces to the average over the centers $\vec{r}_M$ of the cyclotron orbits, i.e., to Eq. (2.11).

In this limit of weak modulations, where the cyclotron orbits are only slightly modified, we may apply Eq. (2.11) also to the case of two-dimensional periodic modulations. However, with increasing modulation strength the nature of the trajectories in the two-dimensional lateral superlattice changes and chaotic trajectories will occur. The velocity along such trajectories will not be a periodic function of time, and the concept of an average (drift) velocity along the trajectory loses its meaning. In such a situation Eq. (B4) is no longer a reasonable approximation to the more general Eq. (B1).

[1] D. Weiss, K. v. Klitzing, K. Ploog, and G. Weimann, Europhys. Lett. **8**, 179 (1989); see also in *High Magnetic Fields in Semiconductor Physics II*, edited by G. Landwehr, Springer Series in Solid-State Sciences Vol. 87 (Springer-Verlag, Berlin, 1989), p. 357.

[2] R. R. Gerhardts, D. Weiss, and K. v. Klitzing, Phys. Rev. Lett. **62**, 1173 (1989).

[3] R. W. Winkler, J. P. Kotthaus, and K. Ploog, Phys. Rev. Lett. **62**, 1177 (1989).

[4] D. Pfannkuche and R. R. Gerhardts, Phys. Rev. B **46**, 12 606 (1992).

[5] C. W. J. Beenakker, Phys. Rev. Lett. **62**, 2020 (1989).

[6] R. R. Gerhardts, Phys. Rev. B **45**, 3449 (1992).

[7] P. Vasilopoulos and F. M. Peeters, Superlatt. Microstruct. **7**, 393 (1990).

[8] D. P. Xue and G. Xiao, Phys. Rev. B **45**, 5986 (1992).

[9] F. M. Peeters and P. Vasilopoulos, Phys. Rev. B **47**, 1466 (1993).

[10] H. A. Carmona *et al.*, Phys. Rev. Lett. **74**, 3009 (1995).

[11] P. D. Ye *et al.*, Phys. Rev. Lett. **74**, 3013 (1995).

[12] S. Izawa, S. Katsumoto, A. Endo, and Y. Iye, J. Phys. Soc. Jpn. **64**, 706 (1995).

[13] J. H. Davies and I. A. Larkin, Phys. Rev. B **49**, 4800 (1994).

[14] P. D. Ye *et al.*, Semicond. Sci. Technol. **10**, 715 (1995).

[15] P. D. Ye and D. Weiss (private communication).

[16] The corresponding result in Eq. (16) of Ref. 8 is too small by a factor 2, due to an incorrect ansatz for the diffusion tensor.

[17] P. H. Beton *et al.*, Phys. Rev. B **42**, 9229 (1990).

[18] J. E. Müller, Phys. Rev. Lett. **68**, 385 (1992).

[19] P. D. Ye *et al.*, Appl. Phys. Lett. **67**, 1441 (1995).

[20] The case of cylinders with a square basis and a homogeneous magnetization in the z direction has been treated by O. Ravel (unpublished).

[21] R. G. Chambers, in *The Physics of Metals, I: Electrons*, edited by J. M. Ziman (Cambridge University Press, London, 1969), p. 175.